Article

Not peer-reviewed version

Developing Models to Predict BRAFV600E and RAS Mutational Status in Papillary Thyroid Carcinoma

Agnes Stephanie Harahap , Imam Subekti , Sonar Soni Panigoro , Asmarinah Asmarinah , Lisnawati Lisnawati , Retno Asti Werdhani , Hasrayati Agustina , Dina Khoirunnisa , Mutiah Mutmainnah , Fajar Lamhot Gultom , Abdillah Hasbi Assadyk , Maria Francisca Ham *

Posted Date: 15 September 2023

doi: 10.20944/preprints202309.1034.v1

Keywords: papillary thyroid carcinoma; BRAF-like; RAS-like; BRAFV600E; RAS mutation; prediction model

Article

Developing Models to Predict *BRAF*V600E and *RAS* Mutational Status in Papillary Thyroid Carcinoma

Agnes Stephanie Harahap [1,2,3,9], Imam Subekti [4], Sonar Soni Panigoro [5], Asmarinah [6], Lisnawati [1], Retno Asti Werdhani [7], Hasrayati Agustina [8], Dina Khoirunnisa [1], Mutiah Mutmainnah [1], Fajar Lamhot Gultom [9,10], Abdillah Hasbi Assadyk [11] and Maria Francisca Ham [1,2,*]

1 Department of Anatomical Pathology, Faculty of Medicine Universitas Indonesia/Dr. Cipto Mangunkusumo Hospital, Jakarta, Indonesia
2 Human Cancer Research Center-Indonesian Medical Education and Research Institute, Faculty of Medicine Universitas Indonesia, Jakarta, Indonesia
3 Doctoral Program in Medical Sciences, Faculty of Medicine Universitas Indonesia, Jakarta, Indonesia
4 Department of Internal Medicine, Faculty of Medicine Universitas Indonesia/Dr. Cipto Mangunkusumo Hospital, Jakarta, Indonesia
5 Department of Surgery, Faculty of Medicine Universitas Indonesia/Dr. Cipto Mangunkusumo Hospital, Jakarta, Indonesia
6 Department of Medical Biology, Faculty of Medicine Universitas Indonesia/Dr. Cipto Mangunkusumo Hospital, Jakarta, Indonesia
7 Department of Community Medicine, Faculty of Medicine Universitas Indonesia, Jakarta, Indonesia
8 Department of Anatomical Pathology, Faculty of Medicine Universitas Padjadjaran/Hasan Sadikin General Hospital, Bandung, Indonesia
9 Department of Anatomical Pathology, MRCCC Siloam Hospital, Jakarta, Indonesia
10 Department of Anatomical Pathology, Faculty of Medicine Universitas Kristen Indonesia, Jakarta, Indonesia
11 Department of Otolaryngology, Head and Neck Surgery, Harapan Kita National Women and Children Health Center, Jakarta, Indonesia
* Correspondence: mariafranciscaham@gmail.com; Tel.: +62818765563

Abstract: The Cancer Genome Atlas (TCGA) has classified papillary thyroid carcinoma (PTC) into indolent RAS-like and aggressive BRAF-like based on its distinct driver gene mutations. This study aimed to assess clinicopathology and pERK1/2 expression variations between BRAF-like and RAS-like PTCs and establish predictive models for *BRAF*V600E and *RAS*-mutated PTCs. A total of 222 PTCs underwent immunohistochemistry staining to assess pERK1/2 expression and Sanger sequencing to analyze the *BRAF* and *RAS* genes. Multivariate logistic regression was employed to develop prediction model. Independent predictors for the *BRAF*V600E mutation include a nuclear score of 3, the absence of capsules, an aggressive histology variant, and pERK1/2 levels exceeding 10% (X2=0.128, P>0.05, AUC=0.734, P<0.001). *RAS* mutation predictive model includes follicular histology variant and pERK1/2 expression >10% (X2=0.174, P>0.05, AUC=0.8, P<0.001). We proposed using the prediction model concurrently with four potential combination group outcomes. PTC cases included in combination of low *BRAF*V600E-scoring group and high *RAS*-scoring group are categorized as RAS-like (adjOR=4.857, P=0.01, 95% CI=1.470-16.049). PTCs included in combination of high *BRAF*V600E-scoring group and low *RAS*-scoring group are categorized as BRAF-like PTCs (adjOR=3.091, P=0.001, 95% CI=1.594-5.995). The different prediction models indicate variations in biological behaviour between BRAF-like and RAS-like PTCs, necessitating adjustments in treatment approaches.

Keywords: papillary thyroid carcinoma; BRAF-like; RAS-like; *BRAF*V600E; *RAS* mutation; prediction model

1. Introduction

Thyroid carcinomas are among the most prevalent malignancies of the endocrine system, with a notable rise in incidence over the last few decades [1]. The emergence of well-differentiated thyroid tumors such as papillary thyroid carcinoma (PTC) and follicular thyroid carcinoma (FTC) has been

 doi:10.20944/preprints202309.1034.v1

linked to alterations in various genes, including *BRAF*, *RAS*, *RET*, and recently discovered gene fusions such as *EIFIAX*, *RET*, *NTRK1/3*, *ALK*, *PAX8-PPARG*, *RGADA*, *FGR2*, and *LTK* genes [2]. PTC, which constitutes 80–85% of overall thyroid carcinoma cases, has particularly received an advanced exploration of its genomic landscape [3]. *BRAF*V600E and *RAS* mutations are the two most prevalent gene mutations detected in PTC, with prevalence rates of 25–82.3% [4,5] and 11.5–20% [3,6,7], respectively. Being mutually exclusive, these driver gene mutations ultimately led to the same incongruous activation of the mitogen-activated protein kinase (MAPK) pathway [8]. This pathway involves the sequential activation and phosphorylation of RAS, RAF, MEK, and ERK, which are important in the regulation of cellular growth and apoptosis. Dysregulation of the gene associated with this pathway can affect cellular function and promote tumorigenesis. Elevated pERK1/2 expression, as detected through immunohistochemistry staining or western blot analysis, has been considered a proxy indicator for heightened MAPK pathway activity in various malignancies [9]. Interestingly, the expression of pERK1/2 has reportedly differed between *BRAF*-mutated and *RAS*-mutated tumors, with the former being more elevated [2]. In addition, *RAS*-mutated PTC demonstrates concurrent activation of P13K/AKT signaling as well as MAPK activation [2]. These signaling differences result in distinct phenotypes of PTCs, which are characterized by varied clinical and histopathological findings.

Among several *BRAF* mutations that have been identified in PTC, *BRAF*V600E constituted most cases. This T1799A point mutation results in the replacement of valine with glutamate and has emerged as a significant clinical determinant due to its association with heightened disease aggressiveness [10]. PTC tumors typically display an inert behavior, with a considerable proportion of patients attaining a survival rate of ten years [11]. However, tumors harboring the *BRAF*V600E were associated with increased mortality rates, higher rates of recurrence, and resistance to radioiodine treatment [12,13]. Several studies have also linked this mutation to various aggressive pathology features, such as perithyroidal extension, node metastases, and advanced clinical stage [14–16]. In contrast to the *BRAF*V600E mutation, tumors possessing the *RAS* mutation were associated with less aggressive pathology characteristics, involving follicular histology variant [12], encapsulated tumors [17], minimal disease invasion [15,18], and lower risk of recurrences [12]. Among the three isoforms of the *RAS* gene, *NRAS* has been known as the most prevalent gene mutation that is closely related to PTC [19]. While it is less common in the American and European populations, *RAS* mutation was reported more frequent in the Asian population [20].

A recent discovery by The Cancer Genome Atlas (TCGA) has been able to classify PTC based on its two major driver gene mutations, which are BRAF-like and RAS-like tumors [2]. Identifying PTCs into BRAF-like and RAS-like tumors during diagnostic work-up is essential, not only for determining the most precise and targeted treatment but also to comprehend the biological behavior between the two. Hence, this study aimed to explore the differences between BRAF-like and RAS-like tumors concerning clinicopathology and pERK1/2 expression and further establish predictive models for *BRAF*V600E and *RAS* mutations in PTC.

2. Materials and Methods

2.1. Study Design and Population

This study retrospectively enrolled PTC patients who had undergone total thyroidectomy at Cipto Mangunkusumo National Hospital and MRCCC Siloam Hospital between January 2019 and September 2022. We excluded cases with aggressive features such as a high mitosis index and necrosis. The clinical information, including age, gender, and clinical stage, was procured from medical records. Three licensed pathologists gathered the histopathological data blindly, involving tumor size, PTC-nuclear score, capsule, histology variant, multifocality, lymphovascular invasion (LVI), extrathyroidal extension (ETE), and node metastases. Histology variants of PTCs were further classified into non-aggressive (classic and follicular) and aggressive (tall cell, oncocytic, and solid) [13].

 doi:10.20944/preprints202309.1034.v1

2.2. pERK1/2 Immunohistochemistry Examination

The expression of pERK1/2 in this present study were classified into high and low expression based on the cut-off point 10% established by Gomes et al [21]. The standard immunohistochemical evaluation procedures were used to assess the expression of pERK1/2. Positive and negative control was included in each specimen. Colon adenocarcinoma paraffin blocks as a positive control were taken from the routine control archives in our institution. Three-mm thickness of unstained slides were cut and rinsed under running water for 2 minutes following deparaffinization and rehydration. In a de-cloaking chamber at a temperature of 96 °C for 25 minutes, antigen retrieval was carried out using pH 9 Tris-EDTA buffer. After 3 minutes of washing in PBS pH 7.4, a blocking solution containing 10% normal horse serum (Thermo Fisher Scientific, Inc.) was administered for 10 minutes at room temperature to block non-specific protein. Each slide was incubated with rabbit monoclonal anti-Phospho-p44/42 MAPK (Erk1/2) (20G11; Cell Signaling Technology, Danvers, MA, USA) at a dilution ratio of 1:600. Subsequently, each slide was incubated with the PolyVue Plus Mouse/Rabbit Enhancer (Diagnostic Biosystems, USA) for 15 minutes followed by PolyVue Plus Mouse/Rabbit HRP Label for 15 minutes. The slides were repeatedly washed before being incubated to diluted diaminobenzidine chromogen buffer substrate for 1 minute at room temperature. Mayer's hematoxylin was used for a 10-second counterstaining procedure at room temperature. Each slide was examined under a light microscope (Leica Microsystems GmbH) and photographed in five representative fields at x400 magnification with a minimum of 500 tumor cells for each case. Tumor cells-stained brown in the nucleus counted as positive. The quantitative evaluation of pERK1/2 expression was performed by counting the proportion of cells stained positively using ImageJ software version 1.51 (National Institutes of Health). The Kappa inter-observer analysis indicated an agreement of 0.879 ($p<0.001$), which is near-perfect.

2.3. Mutational Analysis

The tumor specimens were subjected to mutational analysis using Sanger sequencing to detect BRAFV600E mutation as well as N/H/K-RAS codon 12, 13, and 61 mutations. The procedures were performed according to the methodology outlined in the previous study [22].

2.4. Statistical Analysis

The statistical software package SPSS version 20 was utilized for the purpose of data processing. Bivariate analyses were conducted utilizing the Chi-square and Mann-Whitney U test. Clinicopathological variables that showed a P value <0.05 during bivariate analysis were considered as significant variables and were subsequently added to a multivariate analysis. Binary logistic regression test was employed to conduct the multivariate analysis, utilizing a backward: conditional method. The model's goodness of fit was evaluated by conducting the Hosmer-Lemeshow test. A significance level of 0.05 or higher is indicative of a reliable predictive model. The fittest model results in selected clinicopathological variables which act as the predictor for each BRAFV600E and RAS mutational status. The development of a scoring value for each predictor involved the formulation of the coefficient B and S.E. as displayed in the regression test. Following the implementation of the scoring system for the study sample, an analysis of the receiver operating characteristic (ROC) curve was conducted. An area under the receiver operating characteristic curve (AUC) exceeding 0.7 indicates a satisfactory level of diagnostic precision. The scoring wizard tool was utilized to evaluate the probability of each total score in every predictive model. To evaluate the applicable combinations of BRAFV600E and RAS model prediction, a multinomial logistic regression test and internal validation was performed.

 doi:10.20944/preprints202309.1034.v1

3. Results

3.1. Baseline characteristics

The study retrospectively collected PTC patients who had undergone total thyroidectomy from January 2019 to September 2022, with an initial recruitment of 527 patients. A total of 305 patients were excluded from the study for multiple reasons as illustrated in Figure 1. The study consisted of a total of 222 participants.

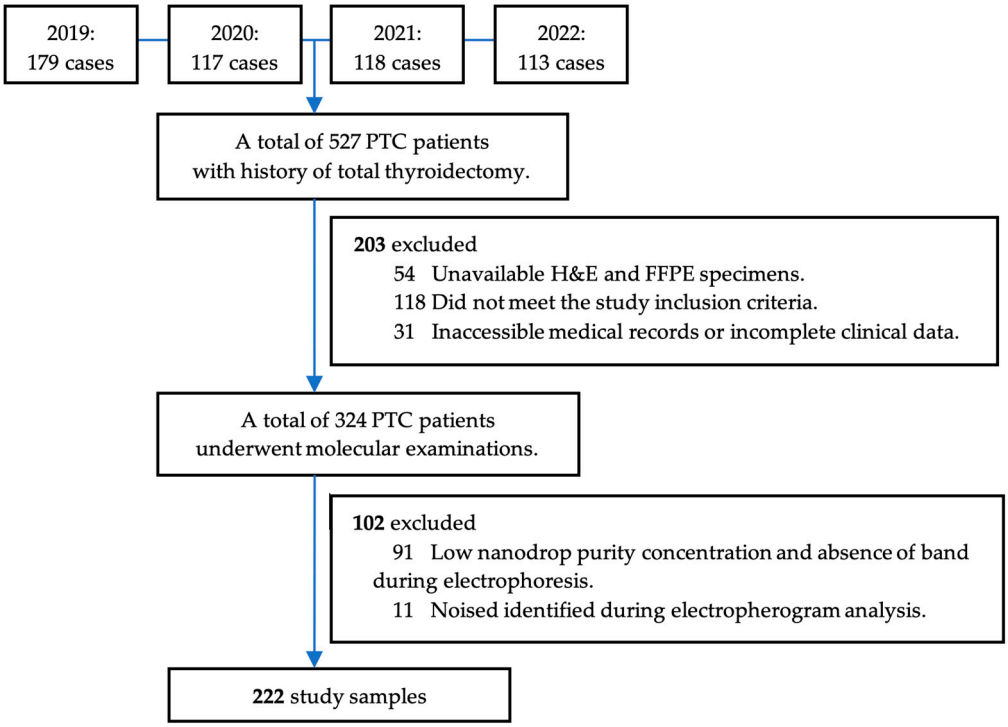

Figure 1. Samples recruitment.

A predominant demographic profile of this study included females (162, 73%), diagnosed under the age of 55 years (163, 73.4%), at clinical stage 1 (166, 74.8%). Histopathological features are dominated by cases characterized by tumor size less than 4 cm (166, 74.8%), nuclear score of 3 (152, 68.5%), lack of capsules (139, 62.6%), non-aggressive variants (152, 68.5%). The histology variants were dominated by follicular variants (87, 39.2%), followed by classic (65, 29.3%), tall cells (52, 23.9%), oncocytic (10, 4.4%), and solid (7, 3.2%), respectively. The presence of multifocality (168, 75.7%), absence of LVI (135, 60.8%), lack of ETE (158, 71.2%), and lack of node metastases (134, 60.4%) constituted the majority of cases in this study. The expression of pERK 1/2 was quantified to range from 0.2% to 99%, with a median value of 5%. Based on the 10% cut off point [21], this study was dominated with low pERK1/2 expression (145, 65.3%).

3.2. Bivariate analysis: correlation between clinico-histopathology characteristics with BRAFV600E and RAS mutational status

One hundred and sixteen cases that did not exhibit the BRAFV600E and RAS mutation are further designated as control. Two distinct bivariate analyses were performed to compare the BRAFV600E-mutated and control, as well as the RAS-mutated and control. The results were outlined in Tables 1 and 2. The bivariate analysis conducted on BRAFV600E-mutated group revealed a significant correlation between BRAFV600E mutation and nuclear score 3 (P=0.001; OR=4.1; 95% CI=1.7–9.4), the absence of tumor capsules (P=0.001; OR=3.2; 95% CI=1.5–6.7), tall cell variant (P=0.001; OR=8.9; 95% CI=3.5–22.6), aggressive histology variants (P=0.001; OR=2.9; 95% CI=1.5–5.4), the

Preprints (www.preprints.org) | NOT PEER-REVIEWED | Posted: 15 September 2023 doi:10.20944/preprints202309.1034.v1

presence of ETE (P=0.01; OR=2.3; 95% CI=1.2–4.4), the presence of node metastases (P=0.008; OR=2.3; 95% CI=1.2–4.3), and high pERK1/2 expression (P=0.008; OR=2.4; 95% CI=1.2–4.8). There was a significant association between RAS mutation and the follicular histology variant (P=0.001; OR=2.6; 95% CI=1.1–6.2), the non-aggressive histology variants (P=0.001; OR=17; 95% CI=2.2–128.6), as well as high pERK1/2 expression (P=0.001; OR=7.6; 95% CI=3.5–16.7).

Table 1. Correlation between clinico-histopathology characteristics and *BRAF*V600E mutation.

Characteristics	*BRAF*V600E N = 64 (%)	Control N = 116 (%)	*p*	OR	95% CI
Clinical features					
Age (years)					
≥ 55	17 (35.4)	31 (64.4)	0.981[a]	0.992	0.497–1.978
< 55	47 (35.6)	85 (64.4)		1.000	*Reference*
Gender					
Man	18 (36.0)	32 (64.0)	0.938[a]	1.027	0.520–2.028
Woman	46 (35.4)	84 (64.6)		1.000	*Reference*
Clinical stage					
Clinical stage IV	7 (58.3)	5 (41.7)	0.114[b]	2.930	0.879–9.766
Clinical stage III	1 (20)	4 (80)		0.523	0.057–4.824
Clinical stage II	13 (43.3)	17 (56.7)		1.601	0.713–3.592
Clinical stage I	43 (32.3)	90 (67.7)		1.000	*Reference*
Stage group					
Late stage (III–IV)	8 (47.1)	9 (52.9)	0.298[a]	1.698	0.621–4.643
Early stage (I–II)	56 (34.4)	107 (65.6)		1.000	*Reference*
Histopathology features					
Tumor size (cm)					
≥ 4	16 (34.8)	30 (64.2)	0.899[a]	0.956	0.474–1.928
< 4	48 (35.8)	86 (65.2)		1.000	*Reference*
Nuclear score					
3	56 (43.4)	73 (56.6)	**≤ 0.001**[a]	4.123	1.796–9.466
2	8 (15.7)	43 (84.3)		1.000	*Reference*
Capsule					
Absent	52 (44.1)	66 (55.9)	**≤ 0.001**[a]	3.283	1.586–6.794
Present	12 (19.4)	50 (80.6)		1.000	*Reference*
Histology variant					
Solid	2 (33.3)	4 (66.7)		2.938	0.459–18.786
Oncocytic	1 (10)	9 (90)		0.653	0.072–5.878
Classic	21 (37.5)	35 (62.5)	**≤ 0.001**[b]	3.525	1.399–8.885
Tall cell	32 (60.4)	21 (39.6)		8.952	3.532–22.690
Follicular	8 (14.5)	47 (85.5)		1.000	*Reference*
Histology group					
Aggressive	35 (50.7)	34 (49.3)	**≤ 0.001**[a]	2.911	1.544–5.488
Non-aggressive	29 (26.1)	82 (73.9)		1.000	*Reference*
Multifocality					
Present	50 (35.7)	90 (64.3)	0.934[a]	1.032	0.494–2.154
Absent	14 (35.0)	26 (65.0)		1.000	*Reference*
Lymphovascular invasion					
Present	31 (43.1)	41 (56.9)	0.086[a]	1.718	0.924–3.197
Absent	33 (30.6)	75 (69.4)		1.000	*Reference*
Extrathyroidal extension					
Present	28 (49.1)	29 (50.9)	**0.010**[a]	2.333	1.220–4.463
Absent	36 (29.3)	87 (70.7)		1.000	*Reference*

Preprints (www.preprints.org) | NOT PEER-REVIEWED | Posted: 15 September 2023 doi:10.20944/preprints202309.1034.v1

Nodes metastases					
Present	34 (47.2)	38 (52.8)	**0.008**[a]	2.326	1.244–4.349
Absent	30 (27.8)	78 (72.2)		1.000	*Reference*
pERK1/2 expression					
High (>10%)	25 (51)	24 (49)	**0.008**[a]	2.457	1.253–4.820
Low (≤10%)	39 (29.8)	92 (70.2)			*Reference*

[a] Chi-square tests. [b] Man Whitney U tests.

Table 2. Correlation between clinico-histopathology characteristics and *RAS* mutation.

Characteristics	*RAS* mutation N = 42 (%)	Control N = 116 (%)	*p*	OR	95% CI
Clinical factors					
Age (years)					
< 55	31 (26.7)	85 (73.3)	0.947[a]	1.028	0.461–2.291
≥ 55	11 (26.2)	31 (73.8)		1.000	*Reference*
Gender					
Woman	32 (27.6)	84 (72.4)	0.635[a]	1.219	0.538–2.764
Man	10 (23.8)	32 (76.2)		1.000	*Reference*
Clinical stage					
Clinical stage I	33 (26.8)	90 (73.2)	0.981[b]	0.458	0.116–1.811
Clinical stage II	5 (22.7)	17 (77.3)		0.368	0.071–1.915
Clinical stage III	0 (0)	4 (100)		0.556	0.310–0.997
Clinical stage IV	4 (44.4)	5 (55.6)		1.000	*Reference*
Stage group					
Early stage (I–II)	38 (26.2)	107 (73.8)	0.721[a]	0.799	0.232–2.746
Late stage (III–IV)	4 (30.8)	9 (69.2)		1.000	*Reference*
Histopathology factors					
Tumor size (cm)					
< 4	32 (27.1)	86 (72.9)	0.696[a]	1.116	0.490–2.541
≥ 4	10 (25.0)	30 (75.0)		1.000	*Reference*
Nuclear score					
2	19 (30.6)	43 (69.4)	0.353[a]	1.402	0.686–2.867
3	23 (24.0)	73 (76.0)		1.000	*Reference*
Capsule					
Present	22 (30.6)	50 (69.4)	0.302[a]	1.452	0.715–2.948
Absent	20 (23.3)	66 (76.7)		1.000	*Reference*
Histology variant					
Follicular	32 (40.5)	47 (59.5)	**≤ 0.001**[b]	2.648	1.121–6.253
Solid	1 (20)	4 (80)		0.972	0.960–9.799
Oncocytic	0 (0)	9 (100)		1.257	1.082–1.460
Tall cell	0 (0)	21 (100)		1.257	1.082–1.460
Classic	9 (20.5)	35 (79.5)		1.000	*Reference*
Histology group					
Non-aggressive	41 (33.3)	82 (66.7)	**≤ 0.001**[a]	17.000	2.247–128.615
Aggressive	1 (2.9)	34 (97.1)		1.000	*Reference*
Multifocality					
Present	28 (23.7)	90 (76.3)	0.163[a]	0.578	0.266–1.255
Absent	14 (35.0)	26 (65.0)		1.000	*Reference*
Lymphovascular invasion					
Present					
Absent	15 (25.4)	41 (73.2)	0.966[a]	1.016	0.486–2.124

 doi:10.20944/preprints202309.1034.v1

	27 (26.5)	75 (73.5)		1.000	*Reference*
Extrathyroidal extension					
Absent	35 (28.5)	87 (71.3)	0.270[a]	1.667	0.668–4.157
Present	7 (19.4)	29 (80.6)		1.000	*Reference*
Nodes metastasis					
Absent	26 (25.0)	78 (75.0)	0.532[a]	0.792	0.380–1.649
Present	16 (29.6)	38 (70.4)		1.00	*Reference*
pERK1/2 expression					
High (>10%)	28 (53.8)	24 (46.2)	**≤ 0.001**[a]	7.667	3.503-16.778
Low (≤10%)	14 (13.2)	92 (86.8)			*Reference*

[a] Chi-square tests. [b] Man Whitney U tests.

3.3. Multivariate analysis: establishing the BRAFV600E prediction model

A multivariate analysis using logistic regression test was conducted to examine the association between BRAFV600E mutation and multiple variables. Nuclear score of 3, the absence of tumor capsules, aggressive histology variants, and high pERK1/2 expression were identified as predictive factors contributing to the presence of BRAFV600E mutation. As indicated in Table 3, the predictor variables were assessed individually to determine their respective score for the development of a BRAFV600E prediction model. The nuclear score of 3, the lack of tumor capsules, and aggressive histology variants each contribute a score of 1. pERK1/2 expression level exceeding 10% corresponds to a score of 2.

Table 3. Logistic regression of the *BRAF*V600E prediction model.

Variables	B coefficient	SE	Wald	*p*	adjOR	95% CI	B/SE	Score
Nuclear score (3)	1.213	0.480	6.375	0.012	3.364	1.312 – 8.626	2.527	1
Capsule (absent)	0.975	0.412	5.605	0.018	2.651	1.183 – 5.941	2.366	1
Histology group (aggressive)	0.858	0.375	5.218	0.022	2.358	1.130 – 4.921	2.288	1
pERK1/2 (>10%)	1.460	0.410	12.668	≤ 0.001	4.308	1.927 – 9.627	3.560	2

The Hosmer-Lemeshow goodness-of-fit test yielded results indicating that the logistic regression model exhibited a favorable level of calibration (X^2=0.128, P> 0.05). The receiver operating characteristic (ROC) curve's area under the curve (AUC) was determined to be 0.734 with P-value <0.001 and a 95% CI of 0.661-0.807 (Figure 2). This finding suggests that the logistic regression model exhibits a favorable level of discrimination. Probability, sensitivity, and specificity values for every outcome of the overall score was summarized in Table 4. Based on the results of probability analysis, it was determined that the highest probability, amounting to 82%, is associated with a total score of 5. This indicates that if PTC achieves a score of 5, there is an 82% likelihood of the occurrence of the BRAFV600E mutation.

Preprints (www.preprints.org) | NOT PEER-REVIEWED | Posted: 15 September 2023 doi:10.20944/preprints202309.1034.v1

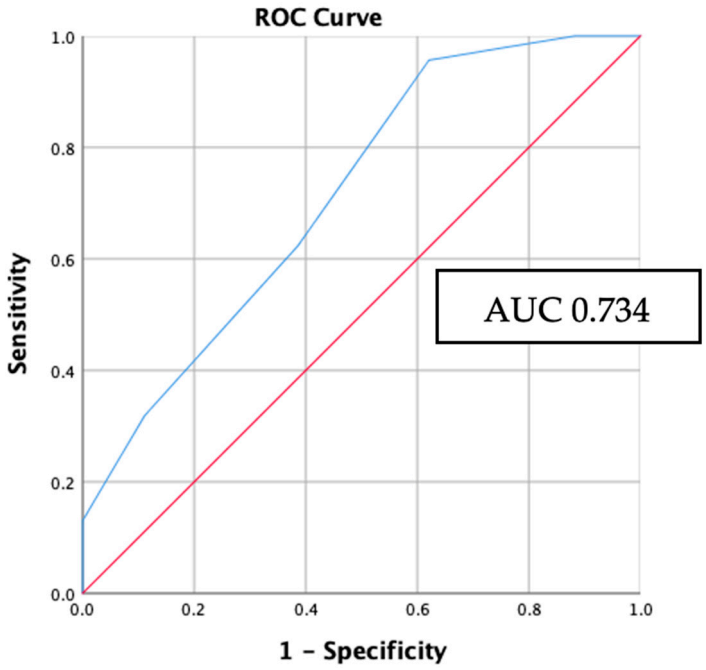

Figure 2. ROC curve of the *BRAF*V600E prediction model.

Table 4. Probability, sensitivity, and specificity of the outcomes of *BRAF*V600E prediction model.

Total score	Probability	Sensitivity	Specificity
0	5%	100%	0%
1	12.33%	100%	12%
2	25.25%	95%	39%
3	43%	63%	65%
4	62%	30%	94%
5	82%	14%	100%

3.4. Multivariate analysis: establishing the RAS mutation prediction model

Based on the multivariate analysis of RAS mutational status, the predictor variables which may be included for the development of the RAS prediction model were follicular histology variant and pERK1/2 expression exceeding 10%. Each corresponding variable gives a score of 1 based on the B/SE value as summarized in Table 5.

Table 5. Logistic regression of the *RAS* mutation prediction model.

Variables	B coefficient	SE	Wald	*p*	adjOR	95% CI	B/SE	Score
pERK1/2 (>10%)	2.101	0.430	23.865	≤ 0.001	8.171	3.518 – 18.981	4.886	1
Variant (follicular)	1.628	0.454	12.877	≤ 0.001	5.092	2.092 – 12.387	3.585	1

The result of the Hosmer-Lemeshow goodness-of-fit test suggests that the RAS mutation-logistic regression model demonstrated a satisfactory level of calibration (X2=0.174, P>0.05). The AUC of the ROC curve was found to be 0.8, with a P-value <0.001 and a 95% CI of 0.702-0.854 (Figure 3). Probability, sensitivity, and specificity values for every outcome of the overall score generated was summarized in Table 6. According to the findings of the probability analysis, it has been ascertained that the highest probability, comprising 70%, is linked to a cumulative score of 2. This suggests that in the case of PTC obtaining a score of 2, there is a probability of 70% for the presence of the RAS mutation.

Preprints (www.preprints.org) | NOT PEER-REVIEWED | Posted: 15 September 2023 doi:10.20944/preprints202309.1034.v1

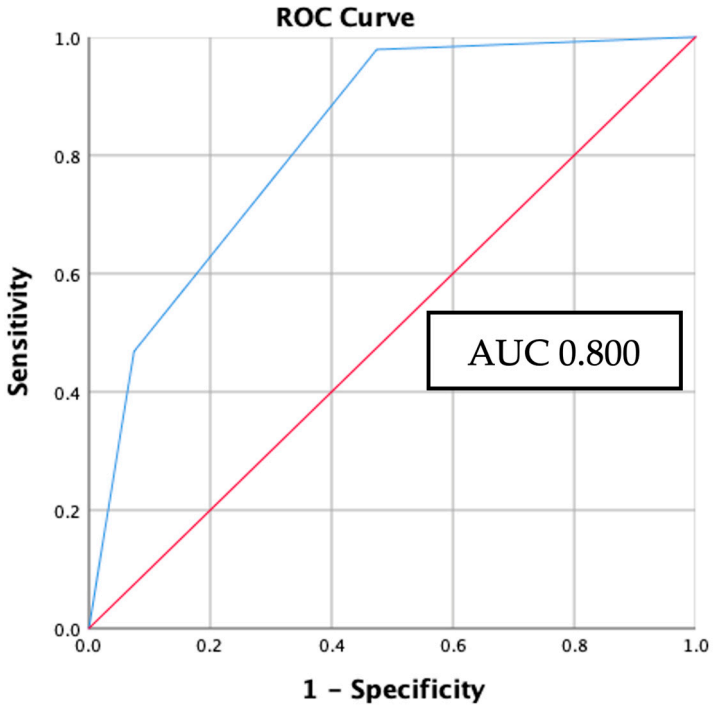

Figure 3. ROC curve of the *RAS* prediction model.

Table 6. Probability, sensitivity, and specificity of the outcomes of *RAS* prediction model.

Total score	Probability	Sensitivity	Specificity
0	5%	100%	0%
1	27%	98%	48%
2	70%	45%	91%

3.5. Internal validation: applicating BRAFV600E and RAS mutation prediction model to study samples

Both prediction models were used to internally validate all study samples. The results showed that a sample capable of fulfilling two prediction models had varying probabilities. Consequently, we established four possible combination outcomes based on the score obtained from the combination of *BRAF*V600E and *RAS* mutation model (Figure 4).

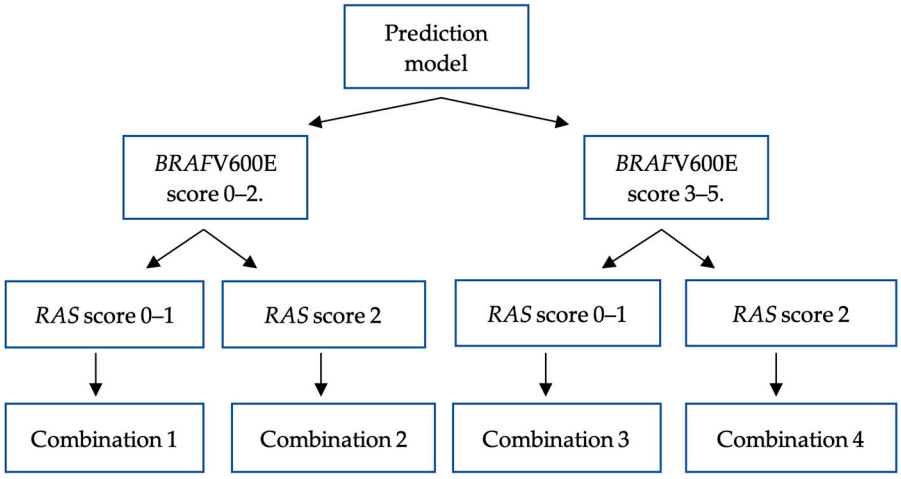

Figure 4. Four combination outcomes of *BRAF*V600E and *RAS* prediction model.

Preprints (www.preprints.org) | NOT PEER-REVIEWED | Posted: 15 September 2023 doi:10.20944/preprints202309.1034.v1

The *BRAF*V600E prediction model results were classified into low *BRAF*V600E-scoring group (total score 0- 2) and high *BRAF*V600E-scoring group (total score 3-5) based on the specificity value of 65% as the middle threshold for identifying the *BRAF*V600E mutational status. The *RAS* prediction model results were classified into low *RAS*-scoring group (total score of 0-1) and high *RAS*-scoring group (total score of 2) using a specificity value of 91%.

Table 7 provides a summary of a multinomial analysis on four combination outcomes. Samples with low *BRAF*V600E-scoring group and low *RAS*-scoring group, as further known as combination 1, acted as the reference group since they had the greatest proportion of non-*BRAF*V600E and non-*RAS* patients. The combination 2 (adjOR=4.857, p=0.01, 95% CI=1.470-16.049), which included samples with low *BRAF*V600E-scoring group and high *RAS*-scoring group, was substantially linked to more occurrences of *RAS* mutation, considered as a RAS-like combination. A strong correlation exists between *BRAF*V600E mutation and combination 3, which includes samples with high *BRAF*V600E-scoring group and low *RAS*-scoring group (adjOR=3.091, p=0.001, 95% CI=1.594-5.995), further considered as BRAF-like combination. The combination 4 group, which contained samples with high *BRAF*V600E-scoring group and high *RAS*-scoring group, was shown to have significantly more *RAS*-mutated patients (adjOR=14.571, p=0.001, 95% CI=4.095-51.855).

Table 7. Multinomial analysis between four combination outcomes and mutational status.

Models outcome	*BRAF*-V600E n (%)	*p*	adj OR	95% CI	*RAS* n (%)	*p*	adj OR	95% CI	Control n (%)
Comb. 1	22 (34.4)	Ref	Ref	Ref	14 (33.3)	Ref	1.00	Ref	68 (58.6)
Comb. 2	2 (3.1)	0.882	0.883	0.171–4.568	**7 (16.7)**	**0.010**	**4.857**	**1.470–16.049**	7 (6)
Comb. 3	**37 (57.8)**	**≤ 0.001**	**3.091**	**1.594–5.995**	9 (21.4)	0.725	1.181	0.467–2.989	37 (31.9)
Comb. 4	3 (4.7)	0.295	2.318	0.481–11.168	**12 (28.6)**	**≤ 0.001**	**14.571**	**4.095–51.855**	4 (3.4)

*Comb. = combination.

4. Discussion

Various genetic alterations have been identified as contributing factors to the development of PTC. The most observed genetic changes in PTC are *BRAF*V600E and *RAS* mutations [23]. These driver gene mutations are mutually exclusive and contribute to the aberrant activation of the MAPK pathway [24]. The different signaling cascades associated with *BRAF*V600E and *RAS* mutations give rise to the specific phenotypic and behavioral characteristics observed in PTC. Tumors harboring *BRAF*V600E mutations exhibit a greater propensity for aggressiveness, characterized by an increased likelihood of disease recurrences [25], mortality [12], and resistance to radio-ablation [13]. Conversely, tumors carrying *RAS* mutations tend to display more indolent behavior [18]. TCGA has emphasized the importance of categorizing PTCs into two distinct subtypes, namely BRAF-like and RAS-like, according to their distinctive biological behaviors [2,26]. This present study aimed to develop a predictive model for *BRAF*V600E and *RAS* mutations in PTC using various histopathological features, including the novel PTC-nuclear score and pERK1/2 expression.

Histopathological factors that are known to contribute to the disease's aggressiveness are the presence of tumor multifocality, vascular invasion, perithyroidal soft tissue invasion, and node metastases [27]. The present study provides more evidence for prior research [28,29] that has established an association between these parameters and the *BRAF*V600E mutation status. A phospho-specific antibody that detects pERK1/2 is also examined in this study to assess the activation of the MAPK pathway on a cellular level. It was documented that pERK1/2 expression exceeding 10% was associated with a higher risk of *BRAF*V600E mutation. Jung et al have discovered a correlation between BRAF-like tumors and high nuclear scores [16]. The findings of this current investigation align with those of a prior study, which demonstrated an association between PTC-nuclear score of 3 and the *BRAF*V600E mutation. We identified three features that emerged as significant predictors of the presence of the *BRAF*V600E mutation. These variables include a nuclear score of 3, the aggressive histology variants, the lack of tumor capsule, and an expression level of pERK1/2 greater

 doi:10.20944/preprints202309.1034.v1

than 10%. The scoring system was established utilizing the characteristics, as indicated in Table 1. The nuclear score of 3, the lack of a tumor capsule, and the aggressive histology variants each contribute a score of 1. If the expression of pERK1/2 exceeds 10%, it is assigned a score of 2. The current research demonstrates a positive correlation between higher total scores and an increased probability of observing a *BRAF*V600E mutation in PTC. The probability of the *BRAF*V600E mutation is highest at 82% when a set of total five scores is taken into account.

In comparison to the *BRAF*V600E mutation, tumors harboring the *RAS* mutation have been linked to a less aggressive pathological phenotype, characterized by a follicular patterned tumor, encapsulated tumors [17], less disease invasion [15,18] and a reduced likelihood of recurrence [18]. Our finding is in line with previous literature, in which *RAS* mutations were significantly more common in the follicular variant of PTCs. Follicular variant of PTCs is considered the non-aggressive histology variants, which comprises most of low-grade tumors. A significant difference between the signaling pathways of *BRAF*V600E-mutated and *RAS*-mutated tumors resides in the lower level of MAPK activity found in *RAS*-mutated tumors [2]. This present study, however, was able to display a significant association between the enhanced MAPK activity in both *BRAF*V600E and *RAS*-mutated PTCs, as displayed in pERK1/2 immunohistochemistry expression. During a multivariate analysis, it was determined that two features, namely the presence of the follicular variant and an expression level of pERK1/2 greater than 10%, were identified as significant predictors for *RAS* mutation. The scoring system was constructed based on the criteria listed in Table 2. Each variable is assigned a value of 1, resulting in a total score of 2, which contributes to a probability of 70% for *RAS* mutation.

The provided study sample exhibits the capacity to satisfy two distinct prediction models with differing probabilities for *BRAF*V600E and *RAS* mutations, posing challenges in determining mutational status. Hence, this work proposes the concurrent utilization of the *BRAF*V600E and *RAS* prediction models in routine clinical applications. All samples were applied to both the *BRAF*V600E and *RAS* prediction models for internal validation. The initial utilization of the *BRAF*V600E prediction model involved its categorization into two distinct groups: a low *BRAF*V600E-scoring group (score 0–2) and a high *BRAF*V600E-scoring group (score 3–5). The *RAS* prediction model consists of two distinct sample groups based on their total scores. One group is characterized by RAS scores ranging from 0 to 1, indicating low *RAS*-scoring group, while the other group has a uniform RAS score of 2, indicating high *RAS*-scoring group. Ultimately, four possible outcomes were established, denoted as combinations within the context of this investigation (Figure 4). There are four possible outcome groups: combination 1 involves cases with low scores in both the *BRAF*V600E and RAS groups, combination 2 involves cases with a low *BRAF*V600E score and a high *RAS* score, combination 3 involves cases with a high *BRAF*V600E score and a low *RAS* score, and combination 4 involves cases with high scores in both the *BRAF*V600E and *RAS* prediction models. The prevalence of combination 1 was seen to be highest among individuals with non-*BRAF*V600E and non-*RAS* mutations. Combination 2 exhibited the highest prevalence in samples where *RAS* mutations were detected, with a statistically significant positive correlation. In combination 3, most of the samples exhibited *BRAF*V600E mutations, which were shown to be statistically significant. Based on the obtained results, it was determined that the dominant parts of combination 2 and combination 3 were RAS-like and *BRAF*V600E-like PTCs, respectively. This discovery provides evidence in favor of the proposed hypothesis. In combination 4, a significant association is shown between *RAS* mutations and a 14-fold increased likelihood compared to non-*BRAF*V600E non-*RAS* mutations. However, no association is found with *BRAF*V600E mutations. On the one hand, this combination exhibits a proclivity toward *RAS* mutations. However, given that PTC with the *BRAF*V600E mutation tends to display a more aggressive nature, it is advisable to approach its interpretation with caution to avoid potential undertreatment. Undertreatment refers to a situation in which PTC has aggressive characteristics, although the management approach is based on low-risk criteria, thereby elevating the likelihood of disease recurrence or metastasis.

Hitherto, this study is the sole research that has constructed a predictive model pertaining to gene mutations in PTC, owing to the routine implementation of molecular examination in developed countries. Our findings can map the histopathology characteristics of PTC into BRAF-like and RAS-

like tumor as a foundation of biological behavior of the tumor. This present study is limited as it does not include other variables such as mortality, recurrence, distant metastases, and therapy response. Additional external validation studies are required to further assess the predictive model, utilizing larger and more diverse samples as well as incorporating additional variables as previously mentioned.

5. Conclusions

Using clinico-histopathology features and pERK1/2 expression, two distinct predictive models for *BRAF*V600E and *RAS* mutational status in PTC were developed. The *BRAF*V600E prediction model consists of a PTC-nuclear score of 3 (score 1), a lack of capsules (score 1), the aggressive histology variants (score 1), and pERK1/2 expression >10% (score 2). The probability of the *BRAF*V600E mutation is highest at 82% when a set of total five scores was reached. The *RAS* prediction model consists of follicular variant (score 1) and pERK1/2 expression > 10% (score 1). BRAF-like tumors are those included in combination 3 (high *BRAF*V600E-scoring group and low *RAS*-scoring group), which exhibits a significant 3-fold increase in the *BRAF*V600E mutation. RAS-like tumors are those belonging to combination 2 (low *BRAF*V600E-scoring group and high *RAS*-scoring group) which possess a significant 4.8-fold increase in *RAS* mutation. These prediction models may serve as a fundamental basis for comprehending the distinct phenotypic and molecular characteristics of BRAF-like and RAS-like PTCs.

Author Contributions: Conceptualization, A.S.H., I.S., S.S.P., R.A. and D.K.; methodology, A.S.H., R.A., D.K., S.S.P. and A.H.A.; validation, A.S.H., M.F.H., L. and F.L.G.; formal analysis, A.S.H., R.A., D.K. and M.M.; resources, A.S.H., L. and F.L.G.; data curation, A.S.H., A., L. and F.L.G.; writing—original draft preparation, A.S.H., D.K. and A.H.A.; writing—review and editing, I.S., S.S.P., M.F.H., A., L., R.A., H.A., F.L.G. and A.H.A.; supervision, I.S., S.S.P. and M.F.H.; funding acquisition, M.F.H. All authors have read and agreed to the published version of the manuscript.

Funding: This study was funded by Universitas Indonesia-Publikasi Terindeks Internasional (PUTI), grant number NKB-1298/UN2.RST/HKP.05.00/2020.

Institutional Review Board Statement: The study was conducted in accordance with the Helsinki Declaration and was authorized by the Institutional Research Ethics Committee of the Faculty of Medicine, Universitas Indonesia Dr. Cipto Mangunkusumo Hospital (FMUI-220 CMH) with the approval number KET-253/UN2.F1/ETIK/PPM.00.02/2022. An ethical waiver of informed consent from the Institutional Review Board was received with the permission number ND-532/UN2.FI/ETIK/PPM.00.02.2022. This study used existing medical records and pathological specimens that were handled in a way that ensured the identity of each subject remained protected.

Data Availability Statement: The dataset utilized in this study is accessible upon request from the author responsible for correspondence.

Conflicts of Interest: The authors declare no conflict of interest.

References

1. Olson, E.; Wintheiser, G.; Wolfe, K. M.; Droessler, J.; Silberstein, P. T. Epidemiology of Thyroid Cancer: A Review of the National Cancer Database, 2000-2013. *Cureus* **2019**, *11* (2), e4127–e4127. https://doi.org/10.7759/cureus.4127.
2. Agrawal, N.; Akbani, R.; Aksoy, B. A.; Ally, A.; Arachchi, H.; Asa, S. L.; Auman, J. T.; Balasundaram, M.; Balu, S.; Baylin, S. B.; Behera, M.; Bernard, B.; Zmuda, E.; Zou, L. Integrated Genomic Characterization of Papillary Thyroid Carcinoma. *Cell* **2014**, *159* (3), 676–690. https://doi.org/10.1016/j.cell.2014.09.050.
3. Jung, C. K.; Little, M. P.; Lubin, J. H.; Brenner, A. V; Wells, S. A.; Sigurdson, A. J.; Nikiforov, Y. E. The Increase in Thyroid Cancer Incidence during the Last Four Decades Is Accompanied by a High Frequency of BRAF Mutations and a Sharp Increase in RAS Mutations. *J Clin Endocrinol Metab* **2014**, *99* (2), E276-85. https://doi.org/10.1210/jc.2013-2503.
4. Xing, M. BRAF Mutation in Thyroid Cancer. *Endocr Relat Cancer* **2005**, *12* (2), 245–262. https://doi.org/10.1677/erc.1.0978.
5. Xie, H.; Wei, B.; Shen, H.; Gao, Y.; Wang, L.; Liu, H. BRAF Mutation in Papillary Thyroid Carcinoma (PTC) and Its Association with Clinicopathological Features and Systemic Inflammation Response Index (SIRI). *Am J Transl Res* **2018**, *10* (8), 2726–2736.

6. Brehar, A. C.; Brehar, F. M.; Bulgar, A. C.; Dumitrache, C. Genetic and Epigenetic Alterations in Differentiated Thyroid Carcinoma. *J Med Life* **2013**, *6* (4), 403–408.
7. Marotta, V.; Bifulco, M.; Vitale, M. Significance of RAS Mutations in Thyroid Benign Nodules and Non-Medullary Thyroid Cancer. *Cancers (Basel)* **2021**, *13* (15). https://doi.org/10.3390/cancers13153785.
8. Soares, P.; Trovisco, V.; Rocha, A. S.; Lima, J.; Castro, P.; Preto, A.; Máximo, V.; Botelho, T.; Seruca, R.; Sobrinho-Simões, M. BRAF Mutations and RET/PTC Rearrangements Are Alternative Events in the Etiopathogenesis of PTC. *Oncogene* **2003**, *22* (29), 4578–4580. https://doi.org/10.1038/sj.onc.1206706.
9. Wang, P.; Han, L.; Yu, M.; Cao, Z.; Li, X.; Shao, Y.; Zhu, G. The Prognostic Value of PERK in Cancer and Its Relationship with Immune Cell Infiltration. *Front Mol Biosci* **2021**, *8*, 648752. https://doi.org/10.3389/fmolb.2021.648752.
10. Wan, P. T. C.; Garnett, M. J.; Roe, S. M.; Lee, S.; Niculescu-Duvaz, D.; Good, V. M.; Jones, C. M.; Marshall, C. J.; Springer, C. J.; Barford, D.; Marais, R.; Cancer Genome Project. Mechanism of Activation of the RAF-ERK Signaling Pathway by Oncogenic Mutations of B-RAF. *Cell* **2004**, *116* (6), 855–867. https://doi.org/10.1016/s0092-8674(04)00215-6.
11. Cao, Y.-M.; Zhang, T.-T.; Li, B.-Y.; Qu, N.; Zhu, Y.-X. Prognostic Evaluation Model for Papillary Thyroid Cancer: A Retrospective Study of 660 Cases. *Gland Surg* **2021**, *10* (7), 2170–2179. https://doi.org/10.21037/gs-21-100.
12. Xing, M.; Alzahrani, A. S.; Carson, K. A.; Viola, D.; Elisei, R.; Bendlova, B.; Yip, L.; Mian, C.; Vianello, F.; Tuttle, R. M.; Robenshtok, E.; Fagin, J. A.; Puxeddu, E.; Fugazzola, L.; Czarniecka, A.; Jarzab, B.; O'Neill, C. J.; Sywak, M. S.; Lam, A. K.; Riesco-Eizaguirre, G.; Santisteban, P.; Nakayama, H.; Tufano, R. P.; Pai, S. I.; Zeiger, M. A.; Westra, W. H.; Clark, D. P.; Clifton-Bligh, R.; Sidransky, D.; Ladenson, P. W.; Sykorova, V. Association between BRAF V600E Mutation and Mortality in Patients with Papillary Thyroid Cancer. *JAMA* **2013**, *309* (14), 1493–1501. https://doi.org/10.1001/jama.2013.3190.
13. WHO Classification of Tumours Editorial Board. *Endocrine and neuroendocrine tumours*. Lyon (France): International Agency for Research on Cancer. https://tumourclassification.iarc.who.int/chapters/53 (accessed 2023-01-24).
14. Li, C.; Lee, K. C.; Schneider, E. B.; Zeiger, M. A. BRAF V600E Mutation and Its Association with Clinicopathological Features of Papillary Thyroid Cancer: A Meta-Analysis. *Journal of Clinical Endocrinology and Metabolism* **2012**, *97* (12), 4559–4570. https://doi.org/10.1210/jc.2012-2104.
15. Adeniran, A. J.; Zhu, Z.; Gandhi, M.; Steward, D. L.; Fidler, J. P.; Giordano, T. J.; Biddinger, P. W.; Nikiforov, Y. E. Correlation between Genetic Alterations and Microscopic Features, Clinical Manifestations, and Prognostic Characteristics of Thyroid Papillary Carcinomas. *Am J Surg Pathol* **2006**, *30* (2), 216–222. https://doi.org/10.1097/01.pas.0000176432.73455.1b.
16. Jung, C. K.; Bychkov, A.; Song, D. E.; Kim, J. H.; Zhu, Y.; Liu, Z.; Keelawat, S.; Lai, C. R.; Hirokawa, M.; Kameyama, K.; Kakudo, K. Molecular Correlates and Nuclear Features of Encapsulated Follicular-Patterned Thyroid Neoplasms. *Endocrinology and Metabolism* **2021**, *36* (1), 123–133. https://doi.org/10.3803/ENM.2020.860.
17. Rivera, M.; Ricarte-Filho, J.; Knauf, J.; Shaha, A.; Tuttle, M.; Fagin, J. A.; Ghossein, R. A. Molecular Genotyping of Papillary Thyroid Carcinoma Follicular Variant According to Its Histological Subtypes (Encapsulated vs Infiltrative) Reveals Distinct BRAF and RAS Mutation Patterns. *Modern Pathology* **2010**, *23* (9), 1191–1200. https://doi.org/10.1038/modpathol.2010.112.
18. Schulten, H.-J.; Salama, S.; Al-Ahmadi, A.; Al-Mansouri, Z.; Mirza, Z.; Al-Ghamdi, K.; Al-Hamour, O. A.; Huwait, E.; Gari, M.; Al-Qahtani, M. H.; Al-Maghrabi, J. Comprehensive Survey of HRAS, KRAS, and NRAS Mutations in Proliferative Thyroid Lesions from An Ethnically Diverse Population. *Anticancer Res* **2013**, *33* (11), 4779 LP – 4784.
19. Hara, H.; Fulton, N.; Yashiro, T.; Ito, K.; DeGroot, L. J.; Kaplan, E. L. N-Ras Mutation: An Independent Prognostic Factor for Aggressiveness of Papillary Thyroid Carcinoma. *Surgery* **1994**, *116* (6), 1010–1016.
20. Odate, T.; Oishi, N.; Vuong, H. G.; Mochizuki, K.; Kondo, T. Genetic Differences in Follicular Thyroid Carcinoma between Asian and Western Countries: A Systematic Review. *Gland Surg* **2020**, *9* (5), 1813–1826. https://doi.org/10.21037/gs-20-356.
21. Gomes, C. C.; Gayden, T.; Bajic, A.; Harraz, O. F.; Pratt, J.; Nikbakht, H.; Bareke, E.; Diniz, M. G.; Castro, W. H.; St-Onge, P.; Sinnett, D.; Han, H.; Rivera, B.; Mikael, L. G.; De Jay, N.; Kleinman, C. L.; Valera, E. T.; Bassenden, A. V; Berghuis, A. M.; Majewski, J.; Nelson, M. T.; Gomez, R. S.; Jabado, N. TRPV4 and KRAS and FGFR1 Gain-of-Function Mutations Drive Giant Cell Lesions of the Jaw. *Nat Commun* **2018**, *9* (1), 4572. https://doi.org/10.1038/s41467-018-06690-4.
22. Harahap, A. S.; Subekti, I.; Panigoro, S. S.; Asmarinah; Lisnawati; Werdhani, R. A.; Agustina, H.; Khoirunnisa, D.; Mutmainnah, M.; Salinah; Siswoyo, A. D.; Ham, M. F. Profile of BRAFV600E, BRAFK601E, NRAS, HRAS, and KRAS Mutational Status, and Clinicopathological Characteristics of Papillary Thyroid Carcinoma in Indonesian National Referral Hospital. *Appl Clin Genet* **2023**, *16*, 99–110. https://doi.org/10.2147/TACG.S412364.

23. Yip, L.; Nikiforova, M. N.; Yoo, J. Y.; McCoy, K. L.; Stang, M. T.; Armstrong, M. J.; Nicholson, K. J.; Ohori, N. P.; Coyne, C.; Hodak, S. P.; Ferris, R. L.; LeBeau, S. O.; Nikiforov, Y. E.; Carty, S. E. Tumor Genotype Determines Phenotype and Disease-Related Outcomes in Thyroid Cancer: A Study of 1510 Patients. *Ann Surg* **2015**, *262* (3), 519–525; discussion 524-5. https://doi.org/10.1097/SLA.0000000000001420.
24. Maik-Rachline, G.; Hacohen-Lev-Ran, A.; Seger, R. Nuclear ERK: Mechanism of Translocation, Substrates, and Role in Cancer. *Int J Mol Sci* **2019**, *20* (5), 1194. https://doi.org/10.3390/ijms20051194.
25. Lee, A. W.; Mendoza, R. A.; Aman, S.; Hsu, R.; Liu, L. Thyroid Cancer Incidence Disparities among Ethnic Asian American Populations, 1990–2014. *Ann Epidemiol* **2022**, *66*, 28–36. https://doi.org/10.1016/j.annepidem.2021.11.002.
26. Jung, C. K.; Bychkov, A.; Song, D. E.; Kim, J.-H.; Zhu, Y.; Liu, Z.; Keelawat, S.; Lai, C.-R.; Hirokawa, M.; Kameyama, K.; Kakudo, K. Molecular Correlates and Nuclear Features of Encapsulated Follicular-Patterned Thyroid Neoplasms. *Endocrinol Metab (Seoul)* **2021**, *36* (1), 123–133. https://doi.org/10.3803/EnM.2020.860.
27. Haugen, B. R.; Alexander, E. K.; Bible, K. C.; Doherty, G. M.; Mandel, S. J.; Nikiforov, Y. E.; Pacini, F.; Randolph, G. W.; Sawka, A. M.; Schlumberger, M.; Schuff, K. G.; Sherman, S. I.; Sosa, J. A.; Steward, D. L.; Tuttle, R. M.; Wartofsky, L. 2015 American Thyroid Association Management Guidelines for Adult Patients with Thyroid Nodules and Differentiated Thyroid Cancer: The American Thyroid Association Guidelines Task Force on Thyroid Nodules and Differentiated Thyroid Cancer. *Thyroid* **2016**, *26* (1), 1–133. https://doi.org/10.1089/thy.2015.0020.
28. Pessôa-Pereira, D.; Medeiros, M. F. da S.; Lima, V. M. S.; Silva, J. C. da; Cerqueira, T. L. de O.; Silva, I. C. da; Fonseca, L. E.; Sampaio, L. J. L.; Lima, C. R. A. de; Ramos, H. E. Association between BRAF (V600E) Mutation and Clinicopathological Features of Papillary Thyroid Carcinoma: A Brazilian Single-Centre Case Series. *Arch Endocrinol Metab* **2019**, *63* (2), 97–106. https://doi.org/10.20945/2359-3997000000120.
29. Silver, J. A.; Bogatchenko, M.; Pusztaszeri, M.; Forest, V.-I.; Hier, M. P.; Yang, J. W.; Tamilia, M.; Payne, R. J. BRAF V600E Mutation Is Associated with Aggressive Features in Papillary Thyroid Carcinomas ≤ 1.5 Cm. *Journal of Otolaryngology - Head & Neck Surgery* **2021**, *50* (1), 63. https://doi.org/10.1186/s40463-021-00543-9.